A FIELD-THEORY-BASED TECHNIQUE FOR THE GROUP-DELAY ANALYSIS OF RECTANGULAR WAVEGUIDE FILTERS

Vladimir A. Labay and Jens Bornemann

Laboratory for Lightwave Electronics, Microwaves and Communications (LLiMiC)
Department of Electrical and Computer Engineering
University of Victoria, B.C. Canada V8W 3P6

ABSTRACT

Group delay analysis of rectangular waveguide filters using a rigorous field-theory-based technique is presented. In order to provide an accurate approach for the transmission phase calculation and its derivative with respect to frequency, the procedure includes higher-order mode excitation and interaction effects at all discontinuities involved. The predicted group delay and magnitude responses are compared to measurements on evanescent-mode T-septum bandpass and millimeter-wave E-plane filter prototypes. Results are shown to be in good agreement.

I. INTRODUCTION

Bandpass filters in rectangular waveguide technology are well known for their excellent performance and their simplicity of fabrication in a variety of applications covering a frequency range between 1 GHz and about 200 GHz. The computer-aided analysis and design of such components is commonly carried out by equivalent-circuit approaches, e.g. [1] or, more recently, by rigorous field-theory-based models most of which involve mode-matching techniques [2-6]. While the equivalent-circuit approach becomes less accurate for broadband applications, field-theory-based models do not experience such limitations and, therefore, are increasingly used by design engineers. Group-delay characteristics of waveguide filters are commonly analyzed using equivalent circuits, e.g. [7, 8]. Little attempt has been made so far to extract the group delay information directly from results obtained by rigorous field-theory models.

Therefore, this paper focuses on the group delay analysis of microwave filters using a field-theory-based technique. In order to provide the design engineer with a measure of accuracy, calculated and measured responses are compared for the examples of an evanescent-mode T-septum waveguide filter and a millimeter-wave E-plane filter.

II. THEORY

The field-theory analysis is based on calculating the generalized scattering matrix of the filter by cascading the individual scattering matrices of the basic key-building block discontinuites contained within the filter structures. Since the generalized scattering matrix contains the complex modal transmission and reflection coefficents, group delay information may easily be extracted. The

scattering matrices of the four key-building block elements in the filters under consideration, i.e., douple-plane step, T-septum discontinuity, H-plane bifurcation and the E-plane T-junction, are found by applying the mode-matching method, e.g. [6].

For a structure requiring the consideration of all field components, e.g. the T-septum waveguide filter (Fig. 1b), the electromagnetic field in each longitudinal homogeneous filter section

$$\vec{E} = -\nabla \times \hat{u}_z \psi_e + \frac{1}{j\omega\varepsilon} \nabla \times \nabla \times \hat{u}_z \psi_m \tag{1}$$

$$\vec{H} = \nabla \times \hat{u}_z \psi_m + \frac{1}{j\omega\mu} \nabla \times \nabla \times \hat{u}_z \psi_e \tag{2}$$

are derived from the z-components of the electric (TE) and magnetic (TM) vector potentials,

$$\psi_e(x,y,z) = \sum_{q=1}^{N_e} \sqrt{Z_{eq}}\, \Psi_{eq}(x,y) \left\{ F_{eq} \exp(-jk_{zeq} z) + B_{eq} \exp(+jk_{zeq} z) \right\} \tag{3}$$

$$\psi_m(x,y,z) = \sum_{p=1}^{N_m} \sqrt{Y_{mp}}\, \Psi_{mp}(x,y) \left\{ F_{mp} \exp(-jk_{zmp} z) - B_{eq} \exp(+jk_{zmp} z) \right\} \tag{4}$$

where $F_{e,m}$, $B_{e,m}$ are the wave amplitudes of the forward and backward traveling waves, respectively, k_z are the propagation constants, and Z_e, Y_m are the wave impedances and admittances of TE and TM modes, respectively. Although the same approach is applicable to the filter structure in Fig. 3b, the analyses of this and similar components [4] are often simplified by using only one vector potential, e.g.

$$\vec{E} = -\nabla \times \hat{u}_x \Phi_e\,, \quad \vec{H} = \frac{1}{j\omega\mu} \nabla \times \nabla \times \hat{u}_x \Phi_e \tag{5}$$

$$\Phi_e(x,y,z) = \sum_{q=1}^{N_e} \sqrt{Z_{eq}}\, \Theta_{eq}(x,y) \left\{ F_{eq} \exp(-jk_{zeq} z) - B_{eq} \exp(+jk_{zeq} z) \right\} \tag{6}$$

The cross-section eigenfunctions $\Psi_{e,m}$ or Θ_e which are determined by solving the corresponding boundary-value problem, are normalized so that the power carried by each mode is 1 W for propagating modes, j W for evanescent TE modes, and $-j$ W for evanesent TM modes. While the cross-section eigenfunctions are known for all the homogeneous filter sections of the millimeter-wave E-plane filter [2], numerical techniques have to be employed to determine those of the T-septum resonators in the below-cutoff filter structure [9].

Once the vector potentials for each filter section have been determined, the tangential electric and magnetic field components of two adjacent sections i, i+1 with cross-section areas $A^i > A^{i+1}$ are matched at their common interface, yielding the generalized modal scattering matrix of the discontinuity

$$
\begin{aligned}
\mathbf{S}_{11} &= -\left[\mathbf{I}+\mathbf{M}\mathbf{M}^T\right]^{-1}\left[\mathbf{I}-\mathbf{M}\mathbf{M}^T\right] \\
\mathbf{S}_{12} &= 2\left[\mathbf{I}+\mathbf{M}\mathbf{M}^T\right]^{-1}\mathbf{M} \\
\mathbf{S}_{21} &= \mathbf{M}^T\left[\mathbf{I}-\mathbf{S}_{11}\right] \\
\mathbf{S}_{22} &= \mathbf{I}-\mathbf{M}^T\mathbf{S}_{12}
\end{aligned}
\tag{7}
$$

where

$$
\mathbf{M}=\begin{bmatrix}
diag\left\{\sqrt{Y_{eq}^{i}}\right\}\mathbf{J}^{ee}diag\left\{\sqrt{Z_{eu}^{i+1}}\right\} & \mathbf{0} \\
diag\left\{\sqrt{Y_{mp}^{i}}\right\}\mathbf{J}^{me}diag\left\{\sqrt{Z_{eu}^{i+1}}\right\} & diag\left\{\sqrt{Y_{mp}^{i}}\right\}\mathbf{J}^{mm}diag\left\{\sqrt{Z_{mv}^{i+1}}\right\}
\end{bmatrix}
\tag{8}
$$

In (7) and (8), T means transposed, **I** is the unit matrix, and *diag*{} denotes a diagonal matrix. The coupling matrices are given by

$$
\left(\mathbf{J}^{ee}\right)_{qu}=\int_{A^{i+1}}\left(\nabla\Psi_{eq}^{i}\times\hat{u}_z\right)\left(\nabla\Psi_{eu}^{i+1}\times\hat{u}_z\right)dA \tag{9}
$$

$$
\left(\mathbf{J}^{me}\right)_{pu}=\int_{A^{i+1}}\left(-\nabla\Psi_{mp}^{i}\right)\left(\nabla\Psi_{eu}^{i+1}\times\hat{u}_z\right)dA \tag{10}
$$

$$
\left(\mathbf{J}^{mm}\right)_{pv}=\int_{A^{i+1}}\left(\nabla\Psi_{mp}^{i}\right)\left(\nabla\Psi_{mv}^{i+1}\right)dA \tag{11}
$$

For details on the slightly different derivation of coupling integrals related to the TE^x-mode approach of (5), (6), the reader is referred to [2, 3]. A general analysis of the E-plane T-junction is given in [10].

Finite lengths of each homogeneous filter section my now be included into the scattering matrix of the discontinuity by incoporating the modal propagation exponential functions of a lossless waveguide. These filter sections are then cascaded to form the overall matrix of the filter. Since input and output waveguides are usually operated in the monomode frequency range, only the related complex matrix elements $S_{11}(1,1)$ and $S_{21}(1,1)$ are of interest. The group delay is defined as the derivative of the angle of $S_{21}(1,1)$ with respect to frequency and is numerically approximated by its difference quotient.

III. RESULTS

The dimensions of the two three-resonator prototype filters, which are chosen as examples, have been optimized for connection to standard X-band and Ka-band waveguide circuitry. Figs. 1 compare the calculated and measured performances of the X-band T-septum evanescent-mode filter centered at 8.8 GHz. Close agreement is obtained not only for return and insertion loss (Fig. 1a) but also for the group delay behavior (Fig. 1b). Note that the measured group delay is almost symmetric and constant throughout approximately half the filter bandwidth. The slight deviations from the theoretical values are mainly attributed to an off-centre location of the below-cutoff guide.

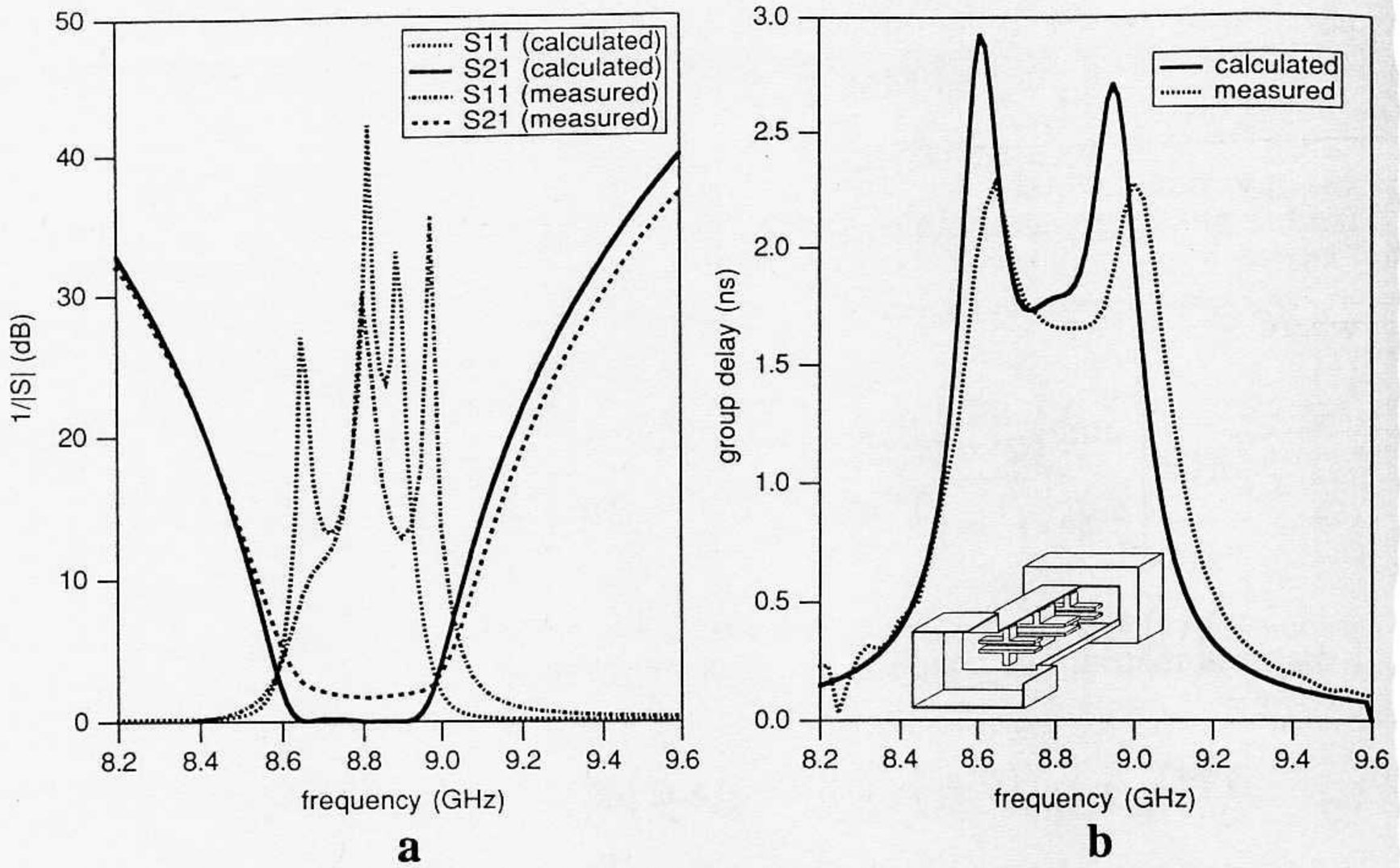

Fig. 1 Measured and calculated characteristics of a three-resonator T-septum evanescent-mode waveguide filter for X-band applications; (a) insertion and return loss, (b) group delay.

Figs. 2 show a five-resonator structure for comparison with Figs. 1. Note that not only the skirt selectivity and stopband attenuation is significantly improved, but the group delay has been increased by the longer overall length of the filter, as it could be expected by adding two resonators.

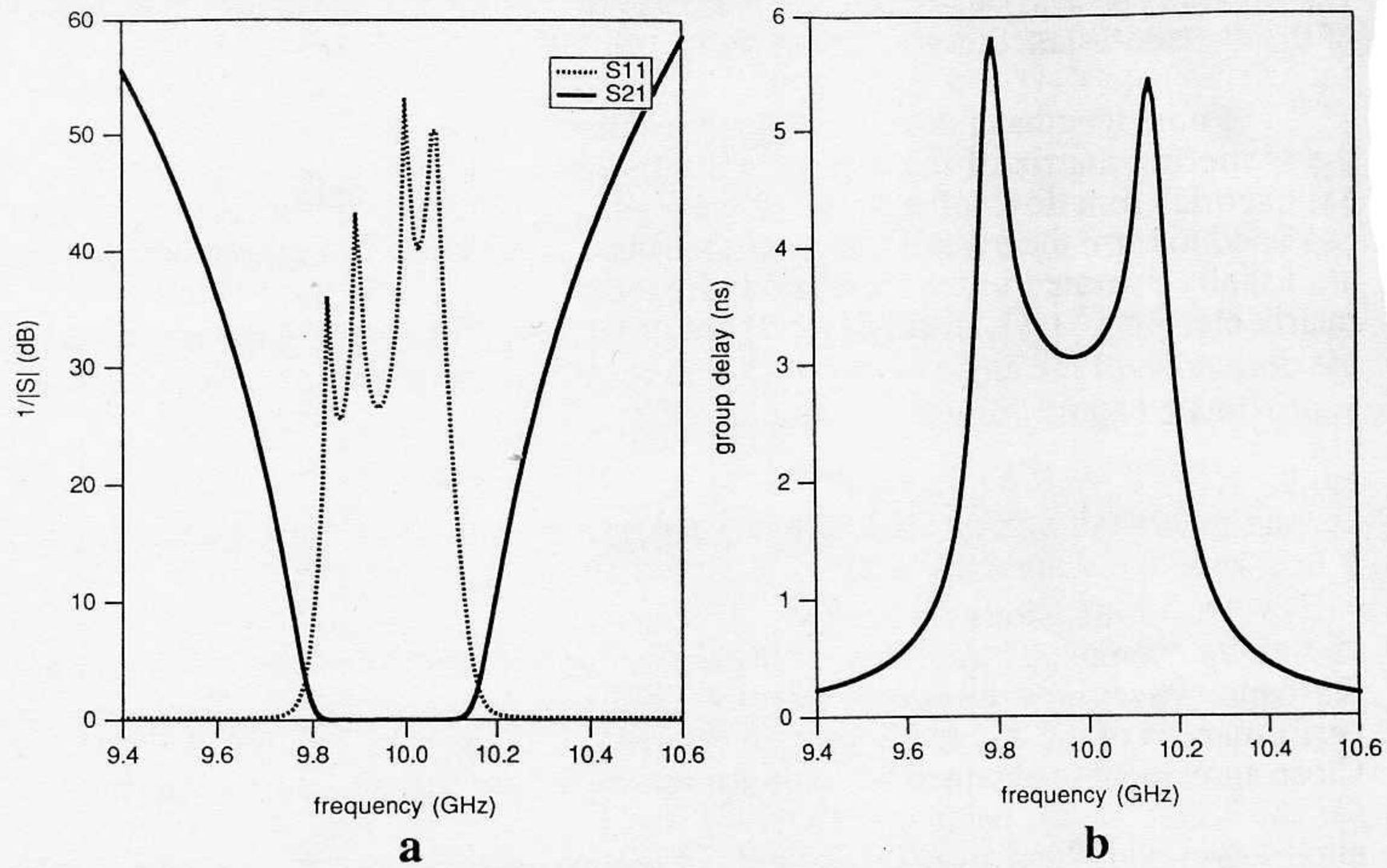

Fig. 2 X-band five-resonator evanescent-mode T-septum waveguide filter; (a) insertion and return loss, (b) group delay.

Figs. 3 demonstrate excellent agreement between the measured and predicted responses of the Ka-band metal insert filter. The minimum insertion loss is 1.5 dB, and stopband poles are beyond 80 dB (Fig. 3a). Although this filter has not been optimized for group delay performance, the close agreement with the calculated values (Fig. 3b) verifies the field-theoretical approach and demonstrates its achievable phase accuracy in millimeter-wave applications.

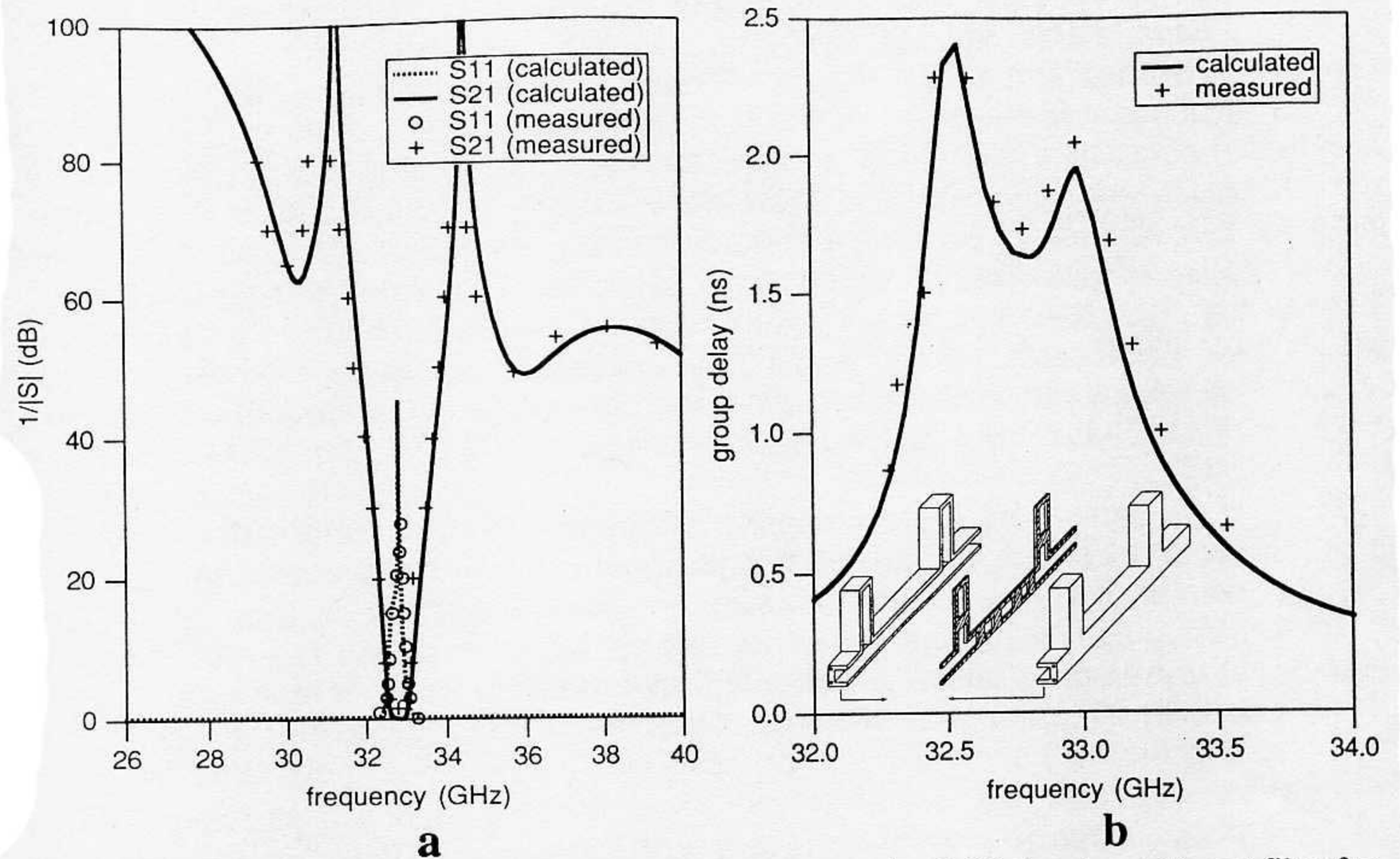

Fig. 3 Measured and calculated characteristics of an extracted-pole Ka-band metal insert filter for millimeter-wave applications; (a) insertion and return loss, (b) group delay.

IV. CONCLUSIONS

A field-theory-based technique for the group delay analysis of rectangular waveguide filters is presented. The theory is verified by measurements on two different microwave/millimeter-wave bandpass filters. Since higher-order mode excitation and interaction effects at all discontinuities involved are taken into account, good agreement between calculations and measurements is obtained, thus demonstrating the achievable phase accuracy in microwave and millimeter-wave computer-aided design applications.

V. REFERENCES

[1] G. Matthaei, L. Young, and E.M.T. Jones, *Microwave Filters, Impedance-Matching Networks, and Coupling Structures*. Dedham, MA: Artech House, 1980.

[2] J. Bornemann, "A new class of E-plane integrated millimeter-wave filters", in *1989 IEEE MTT-S Intl. Microwave Symp. Dig.*, pp. 599-602.

[3] J. Bornemann and R. Vahldieck, "Characterization of a class of waveguide discontinuities using a modified TE^{x}_{mn} mode approach", *IEEE Trans. Microwave Theory Tech.*, vol. 38, pp. 1816-1822, Dec. 1990.

[4] Y.C. Shih and T. Itoh, "E-plane filters with finite-thickness septa", *IEEE Trans. Microwave Theory Tech.*, vol. MTT-31, pp. 1009-1012, Dec. 1983.

[5] Q. Zhang and T. Itoh, "Computer-aided design of evanescent-mode waveguide filter with nontouching E-plane fins", *IEEE Trans. Microwave Theory Tech.*, vol. MTT-36, pp. 404-412, Jan. 1988.

[6] J. Bornemann and F. Arndt, "Transverse resonance, standing wave, and resonator formulation of the ridge waveguide eigenvalue problem and its application to the design of E-plane finned waveguide filters", *IEEE Trans. Microwave Theory Tech.*, vol. MTT-38, pp.1104-1113, Dec 1990.

[7] J.D. Rhodes, "The design and synthesis of a class of microwave bandpass linear phase filters", *IEEE Trans. Microwave Theory Tech.*, vol. MTT-17, pp. 189-204, Apr. 1969.

[8] G. Pfitzenmaier, "Synthesis and realization of narrow-band canonical microwave bandpass filters exhibiting linear phase and transmission zeros", *IEEE Trans. Microwave Theory Tech.*, vol. MTT-30, pp. 1300-1311, Sep. 1982.

[9] V.A. Labay and J. Bornemann, "Singular value decomposition improves accuracy and reliability of T-septum waveguide field-matching analysis", *Intl. J. Microwave and Millimeter-wave CAE*, vol. 2, pp. 82-89, Apr. 1992.

[10] T. Sieverding and F. Arndt, "Field theoretic CAD of open or aperture matched T-junction coupled rectangular waveguide structures", *IEEE Trans. Microwave Theory Tech.*, vol. MTT-40, pp. 353-362, Feb. 1992.